Elastic scattering, absorption, and surface-enhanced Raman scattering by concentric spheres comprised of a metallic and a dielectric region

M. Kerker and C. G. Blatchford
Clarkson College of Technology, Potsdam, New York 13676
(Received 3 May 1982)

Elastic scattering by a small inhomogeneous sphere, comprised of two concentric spherical regions, may be abnormally low if the dielectric constant of the external medium is intermediate between those of the two regions. When one of these regions is a metal with a real negative dielectric constant, there may also be very large enhancement of the scattering due to excitation of a dipolar surface plasmon. For a sphere in which the metallic region is silver, the incident radiation can be tuned over a range of optical wavelengths to give a variation of 10^6 in scattering cross section. Such objects may exhibit very large surface-enhanced Raman scattering with excitation profiles sharply dependent upon the relative thickness of the spherical shell.

I. INTRODUCTION

The electromagnetic scattering cross section of a *small* nonabsorbing ellipsoid, coated with a confocal ellipsoidal shell of a second material and oriented with an axis parallel to the electric vector of the linearly polarized incident radiation, is abnormally low for certain combinations of the axial ratios and the dielectric constants. We have termed such objects "invisible bodies" since an electromagnetic probe would only detect them in the near field.[1–4] A similar effect would be obtained with cylindrical objects having elliptical symmetry.

In this paper we call attention to the possibility of either a dramatic diminution or else a dramatic enhancement of the scattering cross section when one of the regions is comprised of a metal having a nearly real negative dielectric constant. Indeed, with a metal such as silver, the wavelength in the optical range can be tuned to give either diminution or enhancement. The enhancement is due to excitation of the dipolar surface plasmon of the metallic region so that just as in the case of homogeneous objects, huge enhancements are to be expected for Raman scattering [surface-enhanced Raman scattering (SERS)] or fluorescence by molecules at or near the surface. The diminution is due to interference between one region that makes a positive contribution to the polarizability and the other region that makes a negative contribution.

II. ABNORMALLY LOW SCATTERING BY CONCENTRIC SPHERES WITH ϵ_1 AND $\epsilon_2 > 0$

The origin of these effects becomes more apparent if we specialize the ellipsoidal object to a pair of concentric spheres. Then the orientation and polarization requirements are relaxed. The scattering efficiency[5] (scattering cross section divided by cross-section area) is

$$Q_{\text{sca}} = (2/\alpha^2) \sum_{n=1}^{\infty} (2n+1)(|a_n|^2 + |b_n|^2) , \tag{1}$$

where $\alpha = 2\pi b/\lambda$ with b the radius of the spherical object, λ the wavelength, and a_n and b_n the scattering coefficients.[6] For $\alpha < 0.3$, Q_{sca} is approximated by dropping all terms except a_1, and this in turn can be represented by a power series in α in which the leading term is[5,7]

$$a_1 \cong \tfrac{2}{3} i\alpha^3 \left[\frac{(\epsilon_2-\epsilon_3)(\epsilon_1+2\epsilon_2)+q^3(2\epsilon_2+\epsilon_3)(\epsilon_1-\epsilon_2)}{(\epsilon_2+2\epsilon_3)(\epsilon_1+2\epsilon_2)+q^3(2\epsilon_2-2\epsilon_3)(\epsilon_1-\epsilon_2)} \right] = \tfrac{2}{3} i\alpha^3 g , \tag{2}$$

where ϵ_1, ϵ_2, and ϵ_3 are the dielectric constants of the core, the concentric shell, and the surrounding medium, respectively, and $q=a/b$ with a the radius of the core.

The scattered field corresponds to that of an oscillating electric dipole with polarizability proportional to a_1. Indeed, the same polarizability is obtained for this object in a uniform electrostatic field.

The condition for abnormally low scattering is that the numerator of a_1 approach zero, i.e.,

$$q^3_{\min}=-\frac{(\epsilon_2-\epsilon_3)(\epsilon_1+2\epsilon_2)}{(2\epsilon_2+\epsilon_3)(\epsilon_1-\epsilon_2)}\ , \tag{3}$$

where $0\leq q\leq 1$. This requires that the dielectric constant of the surrounding medium be intermediate between that of the two regions. The origin of the very low scattering efficiency is now clear. The particle, whose far field can be thought of as arising from an electric dipole, is so contrived that the dielectric regions each make equal contributions of opposite sign to the polarizability. The reader is referred to Refs. 1–4 for further physical discussion of the effect as well as analogous effects in atomic scattering.

III. CONCENTRIC SPHERES HAVING A SHELL WITH $\epsilon_2<0$

The point of departure in this paper is to consider the possibility of abnormally low scattering efficiency when, as in the case of aerosol particles, the dielectric constant of the external medium is unity. Then, in order that the numerator of a_1 disappear, the dielectric constant of one of the regions in the particle must be either a positive fraction or a real negative number. Since metals have a negative dielectric constant at longer wavelengths than the plasma frequency, a metal-coated dielectric sphere offers a physically realizable structure for obtaining abnormally low scattering efficiency.

In Fig. 1(a) the scattering efficiency of a 10-nm radius sphere in a vacuum ($\epsilon_3=1$) with a core having $\epsilon_1=2.25$ and a coating having $\epsilon_2=-7.08$ is plotted versus q. [In this calculation and all others involving an increment in q, the full-series expansion corresponding to Eq. (1) was used. In cases to be discussed in which the wavelength dependence of scattering, absorption, and SERS is considered, the calculation was based on Eq. (2) or a related expression.] The scattering efficiency is very small at $q=0.92$ as predicted by Eq. (3). However, it does not actually become zero because of contributions both from the higher-order terms in the power-series expansion of a_1 as well as contributions from the other multipoles (a_n and b_n) in Eq. (1). The effect is certainly striking. A metallic layer with a thickness of 8% of the total radius and $\epsilon_2=-7.08$ reduces the scattering cross section of a 10-nm glass sphere ($\epsilon_1=2.25$) by nearly 5 orders of magnitude. Thus, the metal acts as a very efficient "antireflecting" coating.

Equally striking is the strong enhancement at $q=0.74$ where $Q_{\rm sca}$ is nearly 5 orders of magnitude greater than for a homogeneous sphere ($\epsilon_2=-7.08$, $q=0$). Just as the minimum stems from the numerator in Eq. (2) becoming zero, the maximum arises because the denominator goes to zero, i.e.,

$$q^3_{\max}=-\frac{(\epsilon_2+2\epsilon_3)(\epsilon_1+2\epsilon_2)}{(2\epsilon_2-2\epsilon_3)(\epsilon_1-\epsilon_2)}\ . \tag{4}$$

This resonance can be attributed to excitation of a dipolar surface plasmon for a cavity comprised of a spherical shell. It depends both upon the dielectric constant and the relative thickness of the shell. For a homogeneous spherical cavity, the resonance conditions requires $\epsilon=-2$ (Refs. 8 and 9); for a spheroidal cavity the resonance depends upon both ϵ and the axial ratio of the spheroid.[10] One would anticipate analogous results with spheroidal shells, ellipsoids, ellipsoidal shells, etc. Indeed, when both regions of a compound body, core, and shell, exhibit resonances there may be rather complicated interactions and splittings of the resonant peaks.[11]

The minimum may occur either when both regions are dielectrics or as in this case when one of the regions is a dielectric and the other is a plasma. The resonance peak, on the other hand, only occurs with plasmas, i.e., the denominator of Eq. (2) cannot go to zero for $0\leq q\leq 1$ when both ϵ_1 and ϵ_2 are positive.

Excitation of the surface plasmon does not cause the polarizability to blow up catastrophically even in the idealized case of a purely real negative value of ϵ_2 because with retention of higher-order terms in the expansion of a_1 there is a second term in the denominator given by[12]

$$(-\alpha^2/10)[(\epsilon_1+2\epsilon_2)(\epsilon_2^2+9\epsilon_2-10)+10q^3(\epsilon_2^2-1)(\epsilon_2-\epsilon_1)+6q^5\epsilon_2(\epsilon_2-1)(6\epsilon_1\epsilon_2-2\epsilon_1^2-4\epsilon_2)/(\epsilon_1+2\epsilon_2)]\ .$$

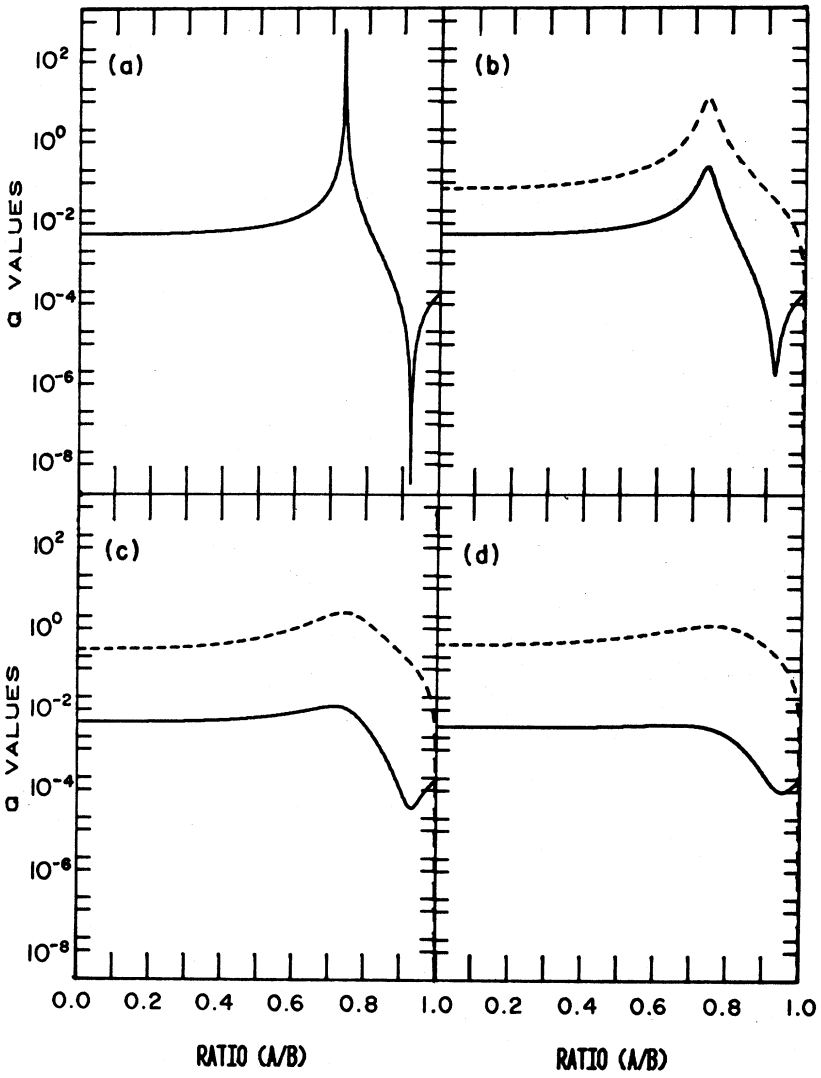

FIG. 1. Scattering efficiency Q_{sca} (solid lines) and absorption efficiency Q_{abs} (dashed lines) for a 10-nm concentric sphere at 450-nm wavelength vs ratio of radii $q=a/b$ for $\epsilon_1=2.25$ and (a) $m_2=0-0.266i$, (b) $m_2=0.05-2.66i$, (c) $m_2=0.30-2.66i$, and (d) $m_2=1.50-2.66i$.

In panels (b)—(d) of Fig. 1, Q_{sca} for this particle is plotted for three complex values of ϵ_2. In fact, the parameter utilized in Figs. 1 and 2 is the refractive index m_2 where $m_2^2=\epsilon_2$. Now, in addition to Q_{sca}, there is loss within the particle which is denoted by the absorption efficiency, Q_{abs}, shown by the dashed line. Q_{abs} increases with increasing real part of m_2. Both maximum and minimum are damped out with increasing real part of m. This is shown in greater detail in Fig. 2.

The absorption and scattering efficiencies, Q_{abs} and Q_{sca}, follow a parallel pattern with increasing q up to q_{max} where the dipolar surface plasmon is excited. Somewhat beyond q_{max} there is the region that exhibits a deep minimum in the scattering. There is no corresponding minimum in the absorption. Rather, Q_{abs} decreases monotonically to $q=1$.

Q_{abs} and Q_{sca} follow a parallel pattern because at low q the particle is mainly metallic, and absorption occurs only in the metallic region. However, with increasing volume of core the out-of-phase contribution of the dielectric core to the polarizability becomes appreciable. The minimum in Q_{sca} arises from destructive interference between the metallic and dielectric regions. Beyond the minimum the contribution of the dielectric core to the polarizability dominates. The volume of metal decreases and so the absorption falls off accordingly.

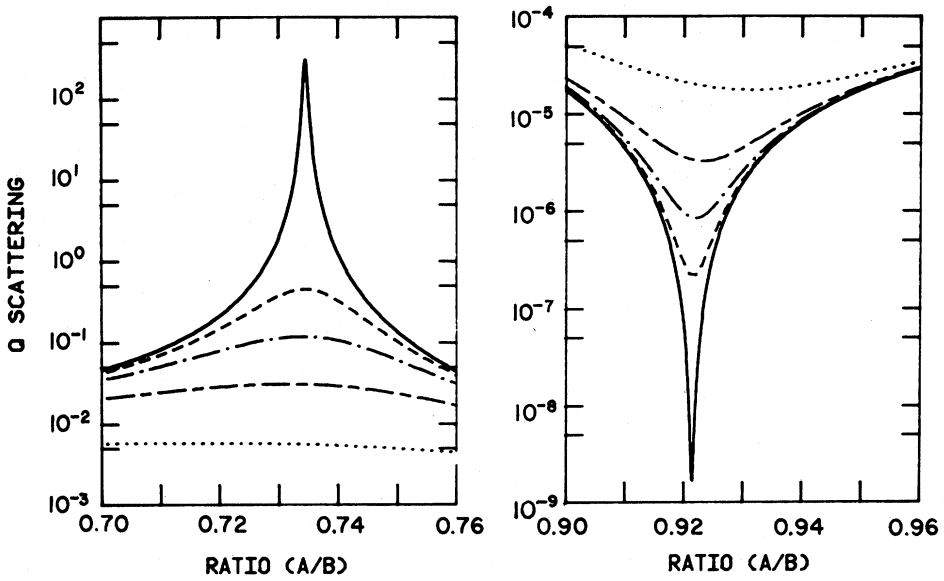

FIG. 2. Same as Fig. 1 in region of maximum and minimum for real part of $m_2=0$ (——), 0.05 (---), 0.10 (—·—·—·), 0.20 (——-), 0.50 (· · ·).

Unlike the scattered radiation, the absorption arises entirely in the metallic region. It depends on the field strength in that region as well as upon the volume of the lossy metal. There is, then, no mechanism for a minimum in Q_{abs} corresponding to the interference mechanism which gives rise to the minimum in Q_{sca}.

In Fig. 3, Q_{sca} and Q_{abs} are plotted versus q for a 10-nm concentric sphere with $\epsilon_1=2.25$, $\epsilon_3=1$, and with values of ϵ_2 obtained from the literature[13] for Ag at $\lambda=335$, 390, 485, and 600 nm. None of the features described above is evident for $\lambda=335$ nm for which $m_2=-0.84-0.30i$. This value deviates too far from the requirement of a purely negative dielectric constant. Also, as noted below, since $|\epsilon_2|<\epsilon_3$, this region no longer makes a negative contribution to the polarizability. In each of the other instances, $m_2=0.05-1.97i$, $0.05-3.00i$, $0.05-4.00i$, sharp maximum and minimum are apparent. Both q_{max} and q_{min} shift to larger values with increasing imaginary refractive index and they become closer to each other. Ag is particularly versatile in exhibiting these maxima and minima since the imaginary part of its dielectric constant is very small from $\lambda=350$ to 1400 nm while its real part varies from -2 to -100 over this wavelength range.

It is of some interest to note that the relative values of q_{max} and q_{min} are independent of the dielectric constant of the core and are determined only by ϵ_2, i.e.,

$$\left[\frac{q_{max}}{q_{min}}\right]^3=\frac{(\epsilon_2+2\epsilon_3)(2\epsilon_2+\epsilon_3)}{2(\epsilon_2-\epsilon_3)^2}\,. \tag{5}$$

This ratio increases from 0 to 1 either as ϵ_2 becomes smaller than -2 or as it increases from -0.5 to 0. Intermediate values of ϵ_2 are inconsistent with having both a maximum and minimum.

In Fig. 4, Q_{sca} and Q_{abs} are plotted versus q for various particle sizes ($b=10$, 20, 60, and 100 nm) for the dielectric constant of Ag reported by Johnson and Christie[13] at 450 nm ($\epsilon_2=-7.07-0.021i$). This illustrates that the sharp maximum and minimum are associated only with a_1 the electric dipolar contribution to Q_{sca}, and are therefore limited to small particles. The secondary peaks on these curves represent the onset of significant contributions from higher multipoles. Thus the secondary peak at $q=0.82$ that becomes more prominent with increasing particle size is due to a quadrupole mode and the peak at $q=0.88$ is due to an octapole mode.

The display in Fig. 5 is comprised of plots of Q_{sca} and Q_{abs} versus wavelength (nm) or energy (eV) for 10-nm radius Ag spheres and $q=0.50$, 0.80, 0.90, and 0.96, using the reported dielectric constant data of Johnson and Christie.[13] The dipolar surface-plasmon resonance for a 10-nm homogeneous sphere ($q=0$) occurs at 3.5 eV. This shifts to 3.25 at $q=0.5$ and to correspondingly lower values with increasing q. The interference minimum that has only begun to develop at $q=0.5$ deepens with in-

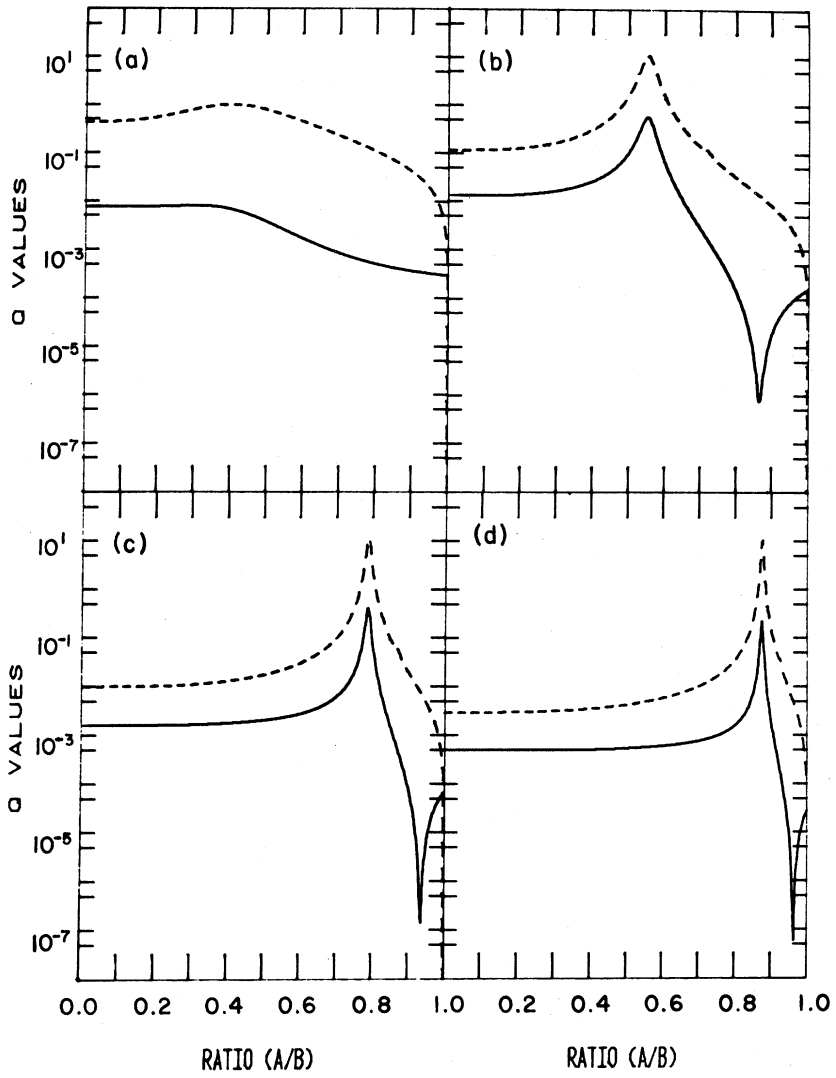

FIG. 3. Q_{sca} and Q_{abs} vs q for a 10-nm concentric sphere, $\epsilon_1=2.25$, $\epsilon_3=1$, and the shell corresponding to Ag at (a) $\lambda=335$ nm, $\epsilon_2=-0.84-0.30i$, (b) $\lambda=390$, $\epsilon_2=-3.88-0.20i$, (c) $\lambda=485$, $\epsilon_2=-9.00-0.30i$, and (d) $\lambda=600$ nm, $\epsilon_2=-16.00-0.40i$.

creasing q and also shifts to lower energy (higher wavelength) in accordance with the requirement of Eq. (5). The shallow minimum at 3.8 eV arises from the dispersion of the refractive index in this region rather than from an interference or a resonance.

Perusal of Fig. 5(c) ($q=0.90$) suggests an interesting possibility for experimental investigation if a system comprised of Ag-coated glass spheres were to be prepared. Q_{sca} would be expected to increase by nearly 10^6 as one tunes from the minimum at 3.0 eV (410 nm) to the maximum at 1.9 eV (650 nm). On the other hand, dielectric spheres of this size would show an eightfold *decrease* of Q_{sca} over this energy range. Whereas a dispersion of these particles would be strongly absorbing and might show a Tyndall beam at 1.9 eV, it would appear less absorbing and quite clear at 3.0 eV.

Figure 6 demonstrates the effect of the refractive index of the medium and of the core upon the resonance maximum and the interference minimum. In Fig. 6(a), increasing the refractive index of the medium shifts the resonance maximum to lower energy, whereas the interference minimum shifts to higher incident energy.[14] However, if the dielectric constant of the core is increased, then both the scattering maximum and minimum are shifted to lower energy as shown in Fig. 6(b).

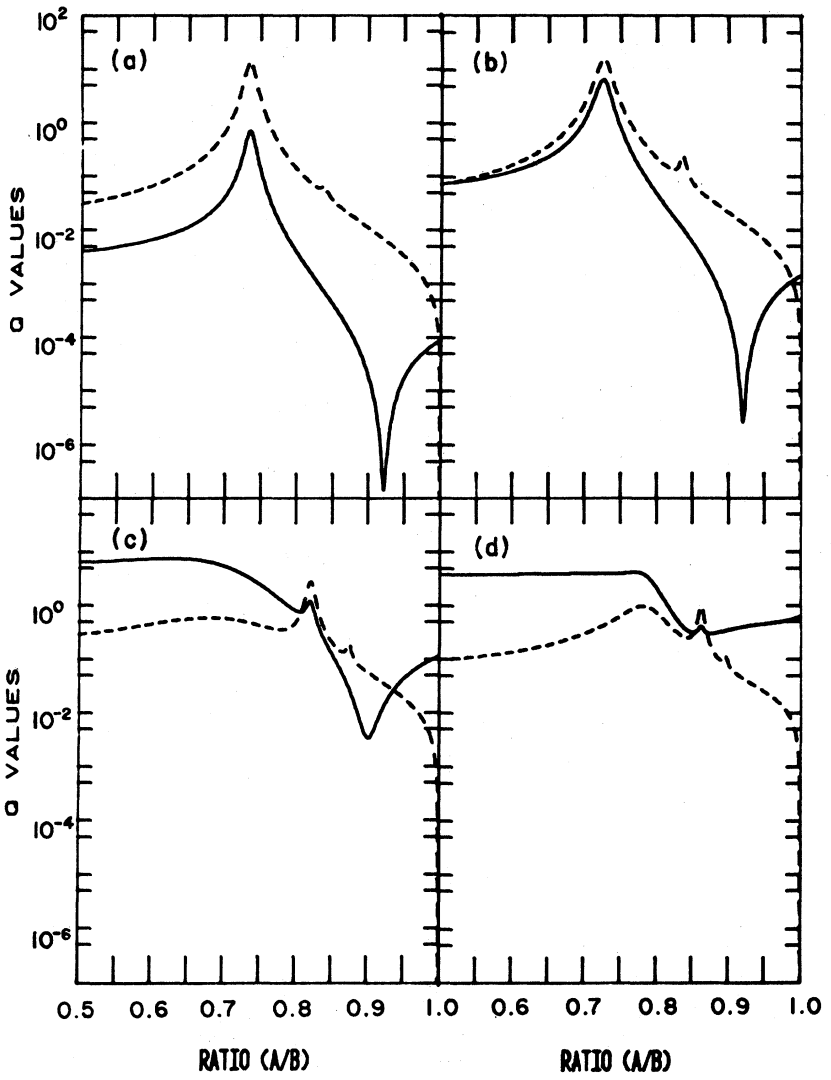

FIG. 4. Q_{sca} and Q_{abs} vs q for (a) $b=10$ nm, (b) $b=20$ nm, (c) $b=60$ nm, and (d) 100-nm radii concentric spheres with $\epsilon_1=2.25$, $\epsilon_3=1$, and $\epsilon_2=-7.07-0.21i$, corresponding to Ag at $\lambda=450$ nm.

A rather interesting aspect is the apparent isobestic point in Fig. 6(a) for which Q_{sca} is independent of ϵ_3. There are two cases for which this may occur. When

$$2q^3(\epsilon_2-\epsilon_1)=\epsilon_1+2\epsilon_2 , \tag{6}$$

it follows from Eq. (2) that $g=-0.5$ and $Q_{sca}=\frac{2}{3}\alpha^4$ for all values of ϵ_3. Since q is constrained to the range 0–1, ϵ_1/ϵ_2 correspondingly ranges from 0 to -2. In Fig. 6(a), for which $q=0.8$ and $\epsilon_1=2.25$, the isobestic point is calculated to occur at $\epsilon_2=-4.67$. Indeed, there is a crossover of the curves obtained by varying ϵ_3 from 1 to 25 which hovers about $\lambda=404$ nm where $\epsilon_2=-4.67-0.22i$ and Q_{sca} ranges within 2% of $(2/3)\alpha^4$ (when the radius is 10 nm). This variation occurs because the experimental dielectric constant of Ag has a finite imaginary part so that the condition that ϵ_1/ϵ_2 be constrained to values from 0 to -2 is not met exactly.

The second case for which an isobestic point may occur requires that

$$q^3(\epsilon_1-\epsilon_2)=\epsilon_1+2\epsilon_2 . \tag{7}$$

Then $g=1$, $Q_{sca}=\frac{8}{3}\alpha^4$, and ϵ_1/ϵ_2 ranges from -2 to $-\infty$. For the same conditions as in Fig. 6(a), i.e., $\epsilon_1=2.25$, $q=0.8$, a second isobestic point would occur at $\epsilon_2=-0.44$. However, such a point

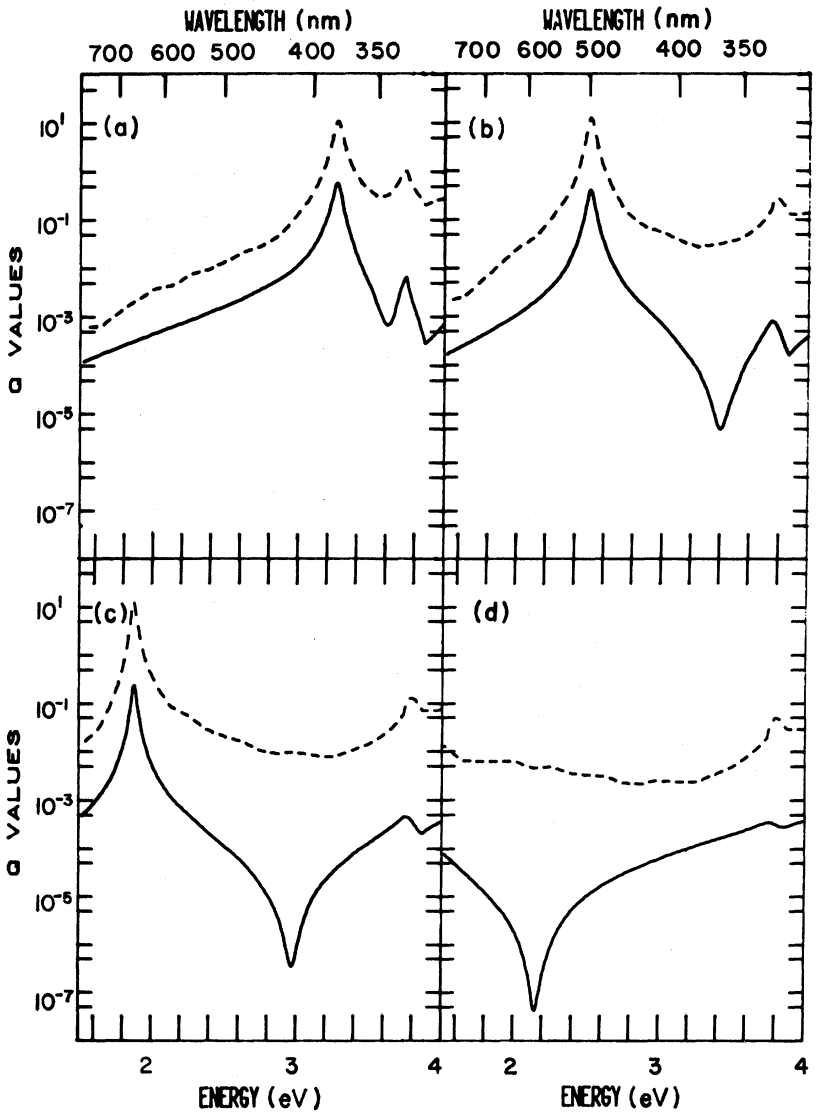

FIG. 5. Q_{sca} and Q_{abs} of a 10-nm radius concentric sphere vs energy of radiation (eV) or wavelength (nm) for (a) $q=0.5$, (b) $q=0.8$, (c) $q=0.9$, and (d) $q=0.96$ for $\epsilon_2=2.25$, $\epsilon_3=1$, and ϵ_2 corresponding to values for Ag.

was not obtained when the values for the dielectric constant of Ag were used for ϵ_2. The real part of the dielectric constant of Ag does become increasingly negative at lower wavelengths, but because the magnitude of the imaginary part also becomes larger, the condition that ϵ_2 be a real negative number is no longer sufficiently satisfied.

IV. CONCENTRIC SPHERES HAVING A CORE WITH $\epsilon_1<0$

We now consider the inverse configuration comprised of a silver core encased in a dielectric concentric spherical shell, i.e., $\epsilon_2>0$ and $\epsilon_1<0$. In this case there is a more severe restriction upon the appearance of the interference minimum than when the Ag comprises the shell. In order that the numerator of Eq. (2) become zero (assuming $\epsilon_2>\epsilon_3$), it is necessary that $\epsilon_1+2\epsilon_2>0$. For glass-coated Ag spheres in a vacuum ($\epsilon_2=2.25$), this condition is met only in the restricted wavelength range 350–380 nm. However, that range may be extended considerably for larger ϵ_2 and so the value $\epsilon_2=9$, corresponding to titanium dioxide, has been used in Fig. 7. In Fig. 7(a), where Q_{sca} is plotted versus q at $\lambda=450$ nm, the interference minimum occurs at a lower value of q than the res-

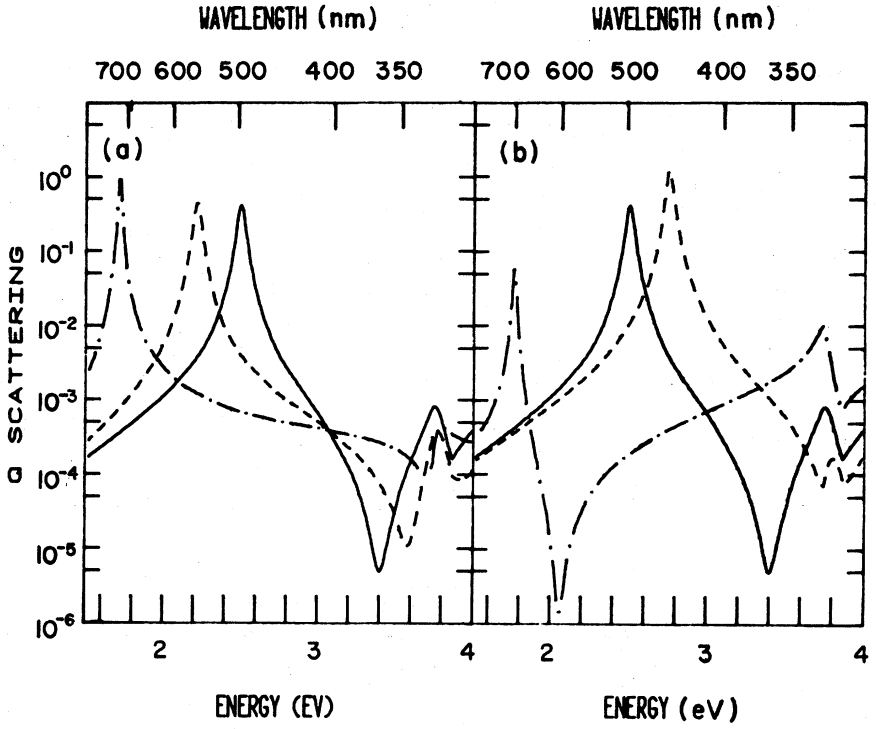

FIG. 6. Q_{sca} of a 10-nm radius concentric sphere with $q=0.8$ vs energy of radiation (eV) or wavelength (nm). The coating is Ag. (a) $\epsilon_1=2.25$, $\epsilon_3=1.00$ (——), 1.77 (— — —), and 4.00 (—·—·—·), (b) $\epsilon_3=1$, $\epsilon_1=1.00$ (— — —), 2.25 (——), 9.0 (—·—·—·).

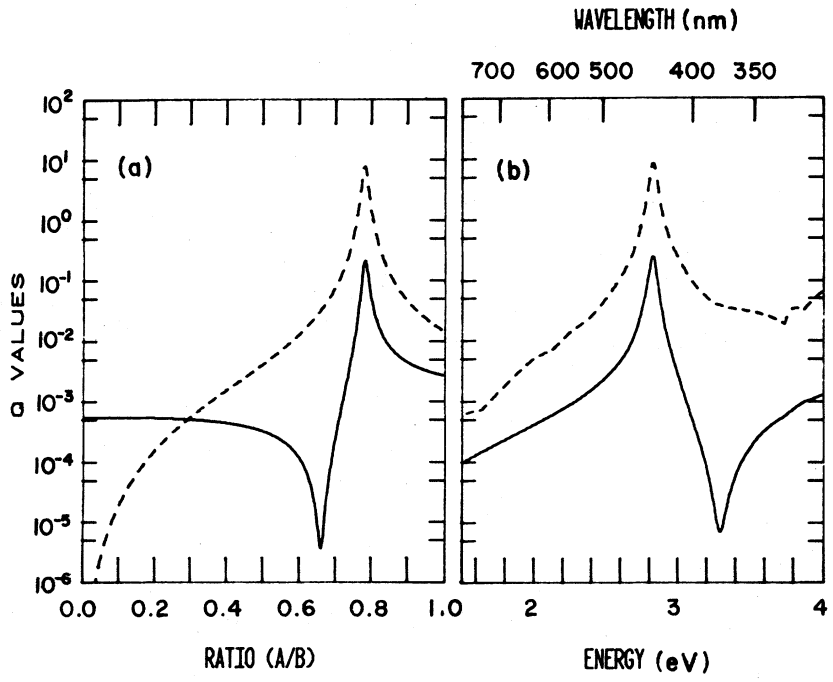

FIG. 7. (a) Q_{sca} and Q_{abs} at $\lambda=450$ nm vs q for a 10-nm radius concentric sphere; Ag core, $\epsilon_2=9$, $\epsilon_3=1$, (b) Q_{sca} and Q_{abs} at $q=0.8$ vs energy (eV) or wavelength (nm). Other conditions as in (a).

onance maximum in contrast to the case treated in the preceding section where Ag comprises the shell instead of the core. Figure 7(b) illustrates that it is possible, provided ϵ_2 is sufficiently large, to tune the incident wavelength so that both the interference minimum and the resonance maximum are obtained, just as when Ag comprises the shell.

The effect of varying the dielectric constant of either the external medium or of the shell for a fixed shell thickness ($q=0.8$) is illustrated in Fig. 8. In Fig. 8(a), the dielectric coating around the silver core is maintained at $\epsilon_2=2.25$ as ϵ_3 varies from 1 to 25. The most striking features are the two isobestic points at 2.35 eV (527 nm) and 3.65 eV (339 nm) corresponding to silver dielectric constants of $-11.5-0.36i$ and $-1.10-0.31i$, respectively. These isobestic points correspond to the conditions specified by Eqs. (6) and (7).

The interference minimum which occurs for $\epsilon_3=25$ requires some discussion. Whereas the earlier minima such as that in Fig. 7(b) result from interference of a region of positive dielectric constant and positive polarization ($\epsilon_2>\epsilon_3$) with a region of negative dielectric constant and negative polarization ($|\epsilon_1|>\epsilon_3$), in this case where ϵ_3 is large, the signs of the polarization in each region are reversed, i.e., $\epsilon_2<\epsilon_3$ and $|\epsilon_1|<\epsilon_3$ are now the respective regions of negative and positive polarization. Unlike the former case [Fig. 7(b)] this interference minimum occurs at a higher wavelength than the resonance maximum. For such a dielectric-coated Ag sphere, there are four interesting features into which one might tune the incident radiation, viz., the interference maximum, the interference minimum, and the two isobestic points.

The curves in Fig. 8(b) correspond to a coated Ag sphere with $q=0.8$ as ϵ_2 varies from 1 to 25, illustrating once again the richly varying optical properties of the dielectric-coated Ag sphere.

V. SURFACE-ENHANCED RAMAN SCATTERING

There is now broad acceptance[15] that the major contribution to surface-enhanced Raman scattering is due to amplification of the local electromagnetic fields upon excitation of surface plasmons of colloidal structures. The Raman scattering molecules respond to these enhanced fields. The colloidal structures may be bumps, pits, ridges, valleys, etc.,

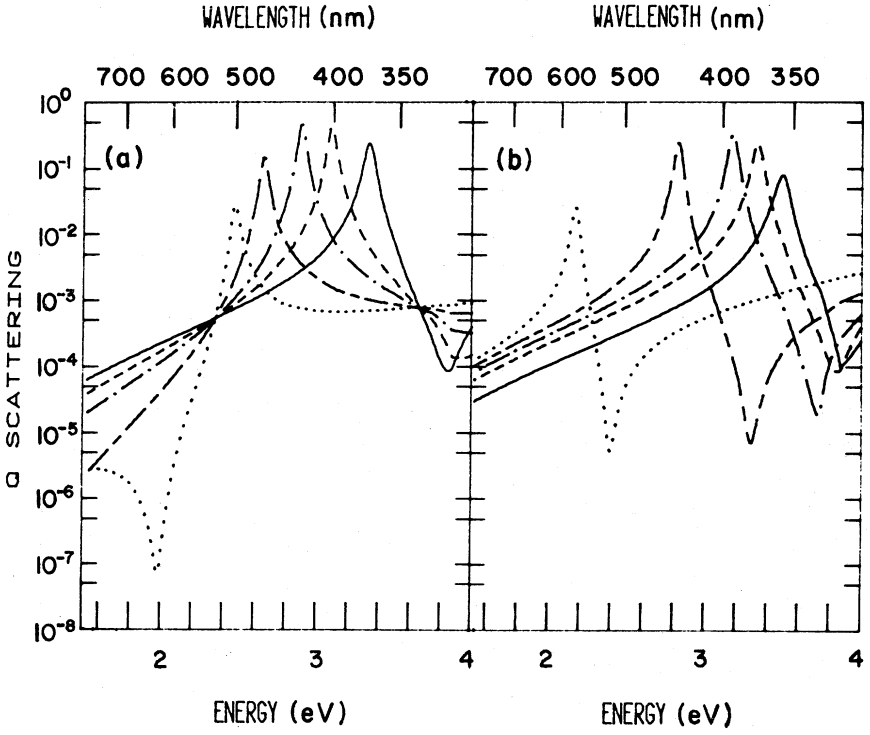

FIG. 8. Q_{sca} of a 10-nm radius concentric sphere vs energy of radiation (eV) or wavelength (nm) for $q-0.8$, Ag core. (a) $\epsilon_2=2.25$, $\epsilon_3=1$ (——), $\epsilon_3=2.25$ (---), $\epsilon_3=4$ (—·—·—·), $\epsilon_3=9$ (———), $\epsilon_3=25$ (· · ·), (b) $\epsilon_3=1$, $\epsilon_2=1$ (——), $\epsilon_2=2.25$ (---), $\epsilon_2=4$ (—·—·—·), $\epsilon_2=9$ (———), $\epsilon_2=25$ (· · ·).

on a macroscopic surface or they may be dispersions of colloidal particles. Creighton, Blatchford, and Albrecht[16] first detected Raman signals from Ag and Au hydrosols and our laboratory has reported enhancements as large as 6×10^5 using Carey-Lea Ag hydrosols.[17] The magnitude and the excitation profiles of such signals have been shown, both experimentally[18,19] and theoretically[8-11] to depend upon size, morphology, and the optical constants of the colloidal particles.

The resonances reported in this paper for metal-coated dielectric spheres or for dielectric-coated metal spheres would also be expected to give rise to SERS. The enhancement can be estimated in the small-particle limit by utilizing an expression derived earlier,[8,9]

$$G=|(1+2g_0)(1+2g)|^2, \tag{8}$$

where g_0 and g, defined in Eq. (2), correspond to values of the dielectric constant at the excitation and Raman wavelengths. The adsorbed Raman scatterers are modeled by a monolayer of dipoles with dipole moments normal to the surface. The enhancement is taken to be the ratio of the Raman signal from an adsorbed dipole to that of a randomly oriented dipole in the medium having the same dipole moment.

We note parenthetically that Eq. (8), which is a limiting value for small particles obtained by reduction of the general boundary-value solution, differs in several respects from another relation proposed for homogeneous spheres,[20] viz.,

$$G=|g_0^4| . \tag{9}$$

Because the effect of dispersion has been neglected, the enhancement estimated by Eq. (9) may be too high by more than an order of magnitude. Also, this expression gives enhancements independent of the magnitude of the Raman shift. Finally, it reduces incorrectly to zero enhancement rather than to unity when ϵ_0 and ϵ_1 becomes close to unity.

In Fig. 9(a), the calculated enhancement is plotted against excitation energy (wavelength) for a Raman scattering monolayer adsorbed on a small sphere comprised of a core with $\epsilon_1=2.25$ and a spherical shell of Ag. The Raman shift is taken as 1010 cm^{-1}. The four curves correspond to $q=0$, 0.50, 0.80, and 0.90. The values for the complex refractive index of Ag have been selected appropriate to each excitation and Raman wavelength.

A number of features are reminiscent of earlier results found for homogeneous metal spheroids.[10] For spheroids the maximum enhancement shifts to longer wavelengths with increasing spheroidal eccentricity. For these concentric spheres there is a similar shift to longer wavelengths as the concentric shell becomes relatively thinner, i.e., as q approaches unity. Also, the region of maximum enhancement is comprised of dual peaks that are separated precisely by the Raman shift. The peak at the higher energy (for a Stokes shift) occurs at the same energy as the absorption band of the particle. As discussed earlier,[10] the higher-energy peak corresponds to the excitation radiation being tuned into the absorption band of the particle. The lower-energy peak corresponds to the Raman shifted radiation being tuned into that band.

The enhancement profiles in Fig. 9(b) are for a Ag core encased in a spherical shell with $\epsilon_2=9.00$ (titanium dioxide). In this case the homogeneous metal particle corresponds to $q=1$, and the enhancement maximum shifts to longer wavelengths with decreasing q. For a homogeneous dielectric sphere ($q=0$), the enhancement is very much smaller but still significant as has been noted earlier.[9] This smaller enhancement is independent of wavelength as shown here only provided ϵ_2 is constant over the wavelength range and most importantly provided the particle is small compared to the wavelength so that only the leading term of Eq. (1) need be used. This result illustrates rather pointedly that the electromagnetic model does not necessarily require direct contact between the metal and the Raman scattering molecules. The experimental observation of SERS by molecules separated from the roughened metal surface by a dielectric layer has been submitted as experimental evidence demonstrating the validity of the electromagnetic model.[21] SERS, luminescence, and absorption effects that occur when the active molecules are embedded in the dielectric coating rather than adsorbed at the outer surface have been treated elsewhere.[11,22,23]

Figures 9(c) and 9(d) are plots of enhancement versus excitation energy for Au- and Cu-coated dielectric spheres. The results are similar to those found for homogeneous metal spheroids. Whereas the maximum enhancement for homogeneous Au and Cu spheres is very much less than that for Ag spheres, the enhancement increases very sharply as spheres comprised of the former materials are distorted to spheroids. Thus eccentric Au and Cu spheroids may exhibit very large enhancements, comparable to those of Ag spheroids. This occurs because the condition for excitation of the dipolar surface plasmon is determined by the shape of the

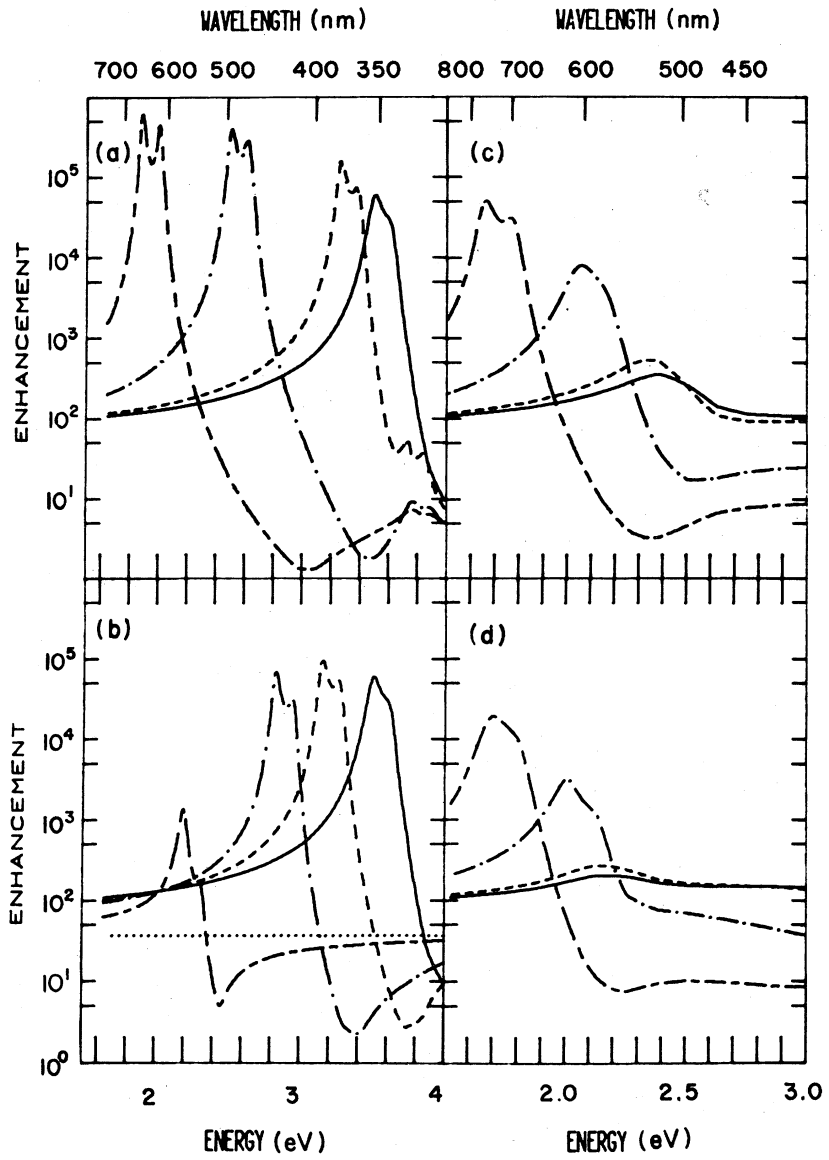

FIG. 9. Enhancement of Raman scattering vs excitation energy (eV) or wavelength (nm) for a monolayer of molecules (electric dipoles) on a small concentric sphere comprised of (a) $\epsilon_1=2.25$, $\epsilon_3=1$, Ag shell, (b) Ag core, $\epsilon_2=9$, ϵ_3-1, (c) $\epsilon_1=2.25$, $\epsilon_3=1$, Au shell, and (d) $\epsilon_1=2.25$, $\epsilon_3=1$, Cu shell. For (a), (c), and (d) the curves correspond to $q=0$ (——), $q=0.50$, (---), $q=0.80$ (—·—·—·), $q=0.90$ (—-—-). For (b) $q=1$ (——), $q=0.90$ (---), $q=0.80$ (—·—·—·), $q=0.50$ (—-—-), $q=0$ (· · ·).

plasma cavity as well as by the values of the optical constants. It is apparent from Figs. 9(c) and 9(d) that similar effects occur with spherical shells of Au and Cu. Although the maximum value of SERS for the homogeneous Au and Cu spheres is only 0.01 that of silver, for $q=0.9$ the enhancement of the Au-coated sphere is 0.10 that of Ag; for Cu it is 0.04 that of Ag.

ACKNOWLEDGMENT

This work was supported by National Science Foundation Grant No. CHE-8011444 and by U.S. Army Research Office Grant No. DAAG-29-79-6-005. We appreciate the suggestion of Professor O. Siiman to explore the connection between the resonance maximum and SERS.

[1]M. Kerker, J. Opt. Soc. Am. 65, 376 (1975).
[2]M. Kerker, D. D. Cooke, and W. D. Ross, J. Paint Technol. 47 (113), 33 (1975).
[3]H. Chew and M. Kerker, J. Opt. Soc. Am. 66, 445 (1976).
[4]M. Kerker and D. D. Cooke, J. Coatings Technol. 48 (125), 35 (1976).
[5]M. Kerker, *The Scattering of Light and Other Electromagnetic Radiation* (Academic, New York, 1969), p. 50.
[6]A. L. Aden and M. Kerker, J. Appl. Phys. 22, 1242 (1951).
[7]A. Güttler, Ann. Phys. (Leipzig) 11, 65 (1952).
[8]D.-S. Wang, H. Chew, and M. Kerker, Appl. Opt. 19, 2256 (1980).
[9]M. Kerker, D.-S. Wang, and H. Chew, Appl. Opt. 19, 4159 (1980). This is a corrected version of the paper on pp. 3373ff., which had been printed without incorporating many corrections.
[10]D.-S. Wang and M. Kerker, Phys. Rev. B 24, 1777 (1981).
[11]D.-S. Wang and M. Kerker, Phys. Rev. B 25, 2433 (1982).
[12]We acknowledge the assistance of Professor Herman Chew who has derived this expression which applies when $\epsilon_3 = 1$.
[13]P. B. Johnson and R. W. Christy, Phys. Rev. B 6, 4370 (1972).
[14]H. C. Van de Hulst, *Light Scattering by Small Particles* (Wiley, New York, 1957), p. 70.
[15]Z. Author in *Surface Enhanced Raman Scattering,* edited by R. K. Chang and T. Furtak (Plenum, New York, 1982).
[16]J. A. Creighton, C. G. Blatchford, and M. G. Albrecht, J. Chem. Soc., 75, 790 (1979).
[17]M. Kerker, O. Siiman, L. A. Bumm, and D.-S. Wang, Appl. Opt. 19, 3253 (1980).
[18]J. A. Creighton, C. G. Blatchford, and J. R. Campbell, Surf. Sci. (in press).
[19]O. Siiman, R. Callaghan, L. A. Bumm, and M. Kerker, in *Proceedings of the Eighth International Conference on Raman Spectroscopy, Ottawa, Canada, 1980,* edited by W. F. Murphy (North-Holland, Amsterdam, 1982).
[20]S. L. McCall, P. M. Platzman, and P. A. Wolff, Phys. Lett. 77A, 381 (1980).
[21]C. A. Murray, D. L. Allara, and M. Rhinewine, Phys. Rev. Lett. 46, 57 (1981).
[22]S. Garoff, D. A. Weitz, T. J. Gramila, and C. D. Hanson, Opt. Lett. 6, 245 (1981).
[23]Z. Kotler and A. Nitzan, J. Phys. Chem. 86, 2011 (1982).